Size-selective encapsulation of C_{60} and C_{60}-derivatives within an adaptable naphthalene-based tetragonal prismatic supramolecular nanocapsule

Cristina García-Simón,[a,†,*] Alba Monferrer,[†,a] Marc Garcia-Borràs,[b] Inhar Imaz,[c] Daniel Maspoch,[c,d] Miquel Costas,[a,*] Xavi Ribas[a,*]

[a.] Dr. C. García-Simón, A. Monferrer, Dr. M. Costas, Dr. X. Ribas, Institut de Química Computacional i Catàlisi (IQCC) and Departament de Química, Universitat de Girona, Campus Montilivi, Girona, E-17003, Catalonia, Spain.

[b.] Dr. M. Garcia-Borràs, Department of Chemistry and Biochemistry, University of California, Los Angeles, CA90095, United States.

[c.] Dr. I. Imaz, Dr. M. Maspoch, Institut Català de Nanociència i Nanotecnologia, ICN2, Campus UAB, 08193 Bellaterra, Catalonia, Spain.

[d.] Dr. D. Maspoch, ICREA, Pg. Lluís Companys 23, 08010 Barcelona, Catalonia, Spain

[†] Equally contributing author.

Novel naphthalene-based $5 \cdot (BArF)_8$ capsule allows for the size-selective inclusion of C_{60} from fullerene mixtures. Its size selectivity towards C_{60} has been rationalized by its dynamic adaptability in solution that has been investigated by Molecular Dynamics. Additionally, $5 \cdot (BArF)_8$ encapsulates C_{60}-derivatives such as C_{60}-PCBM and N-methyl-pyrrolidine-C_{60}. The latter can be separated from C_{60} since $5 \cdot (BArF)_8$ displays distinct affinity between them.

The metal-ligand coordination approach has led to the preparation of sophisticated discrete three-dimensional (3D) structures, which are of great interest due to their intrinsic complexity, which conveys multifunctionality, and potential applications in fields such as molecular catalysis, sensing or purification.[1–3] Indeed, the possibility of tuning the dimensions of the confined space by modifying the 3D molecular structure is an attractive feature to gain control over the guest affinity, and allows for the preparation of extended libraries of coordination capsules.[4,5] On the other hand, purification of fullerenes is remarkable due to their applications in materials science and medicine.[6,7] Even though fullerenes extracts are easily available, the selective purification of a

specific fullerene cage is still a challenging task basically accomplished by means of high performance liquid chromatography (HPLC) techniques, that are generally tedious, time- and energy consuming.[8] Another challenging issue is the separation of parent fullerenes from their corresponding derivatives, which is also mainly restricted to HPLC separation. C_{60}-derivatives such as [6,6]-phenyl C_{61} butyric acid methyl ester (PCBM-C_{60}) or fulleropyrrolidines, present promising applications in material science; but they need to be available in a pure form to display full efficiency.[9,10] To date, numerous examples of 3D molecular receptors based in metal-ligand coordination bonds and capable of hosting fullerenes have been reported.[11–14] However, the separation of a single fullerene by size-confinement effects is not straightforward since the molecular receptors display high affinity for different-sized fullerenes simultaneously.[15] In most reported examples a higher affinity towards C_n ($n \geq 70$) over C_{60} is observed, due to more significant solvophovic effects and the more extended π-surface of larger fullerenes that enhances capsule-fullerene interaction.[16–19] The reverse trend is observed in very limited examples.[20]

Our group previously reported a coordination nanocapsule (**4**·(BArF)$_8$) capable of encapsulating different sized fullerenes from C_{60} to C_{84}.[21] This lack of size selectivity was attributed to its pronounced breathing ability and large cavity size. In light of the importance of C_{60} and its derivatives, herein we report a nanocapsule (**5**·(BArF)$_8$), which bears a smaller cavity, obtained by tuning the length of its spacers. The newly designed nanocapsule with naphthalene spacers is capable of exclusively encapsulating smaller C_{60} fullerene and its corresponding mono-adduct derivatives in a selective manner.

New metallo-capsule **5**·(X)$_8$ (X = CF$_3$SO$_3$, BArF) was synthesized by coordination driven self-assembly of the carboxylate units from Zn^{II}-porphyrin (**2**) and Pd^{II}-based macrocyclic synthons (**Pd-1c**). **5**·(X)$_8$ differs from our previously reported capsules **3**·(X')$_8$ (X'= ClO$_4$, CF$_3$SO$_3$) and **4**·(X)$_8$ in the nature of the hexaaza macrocyclic ligands used to synthesize the ligands (**1b-1c**) and therefore the corresponding Pd^{II}-clip building blocks (Scheme 1).[21,22] Nanocapsule **3**·(X')$_8$ contained a phenyl ring in its macrocyclic ligands (**1**), and the crystallographic distance between its porphyrins was 7.5 Å. On the other hand, **4**·(X)$_8$ included a biphenyl moiety in **1b**, rendering a PorphZn····PorphZn distance of 14.1 Å measured from X-ray structure (Figure 2). While the former capsule **3** was only capable of encapsulating flat anionic π-guests, capsule **4** could host fullerene molecules up to C_{84} with very high association constants (up to $K_a > 10^8$ M^{-1}). For the new nanocapsule **5**·(X)$_8$, which contains 2,6-disubstituted naphthalene units in the macrocyclic ligand (**1c**) (Figures S1-S27) an intermediate capsule-size was envisioned (Scheme 1).
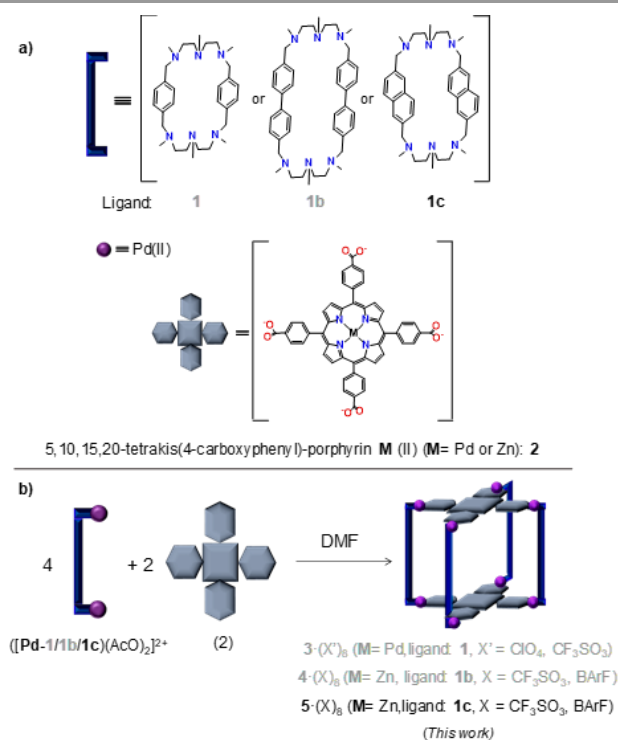
Scheme 1. Schematic representation of the library of coordination nanocapsules **3**-**5**. (a) Spacers used to obtain (b) the tetragonal-prismatic supramolecular capsules **3**•(X')$_8$ (X'= ClO$_4$, CF$_3$SO$_3$), **4**•(X)$_8$ and **5**•(X)$_8$ (X= CF$_3$SO$_3$, BArF) (BArF: tetrakis[3,5-bis(trifluoromethyl)phenyl]borate).

Formation of nanocapsule **5**·(CF$_3$SO$_3$)$_8$ was first confirmed by High Resolution Mass Spectrometry (HRMS) (Figure S28). Then, CF$_3$SO$_3^-$ anions were exchanged by BArF anions to increase its solubility. **5**·(BArF)$_8$ was obtained in good yield, effectively showing an enhanced solubility in different organic solvents, including CH$_3$CN and dichloromethane (DCM). HRMS of **5**·(BArF)$_8$ showed ions corresponding to the cages with consecutive loss of counteranions (Figure 1a and Figure S29), demonstrating its integrity in solution. Full NMR characterization was also performed for **5**·(BArF)$_8$ (Figures S30-36). Remarkably, the DOSY NMR experiment (CH$_3$CN, 298 K) afforded a diffusion coefficient of D = 3.1·10-10 m^{2}s^{-1}, indicating that the dimensions of **5**$^{8+}$ correspond to a hydrodynamic radius of 18.5 Å in solution (Figure S37 and Figure S38), in line with the value estimated from crystallographic data (see below and Figure S38b).

Crystallographic data was obtained from **5**·(CF$_3$SO$_3$)$_8$ crystals at the XALOC beamline of the ALBA Synchrotron (Figure 2a and Supplementary Information for Single-Crystal X-Ray Diffraction - SCXRD details). Nanocapsule **5**$^{8+}$ consists of two parallel tetracarboxylated Zn^{II}-porphyrins linked by four macrocyclic dinuclear Pd^{II} complexes. The four-carboxylate residues of each porphyrin are linked by means

of η^1-O monodentate coordination to one Pd^{II} center (Figure S38). As in 3^{8+} and 4^{8+},[19,20] 5^{8+} presents a tetragonal prismatic geometry bearing a D$_4$ symmetry. The crystallographic PorphZn···PorphZn distance in $5 \cdot (CF_3SO_3)_8$ is 8.2 Å. As expected, this distance lays between the observed in capsules $3 \cdot (X')_8$ and $4 \cdot (X)_8$ (see Scheme 1 and Figure 2a). In light of the size contraction with respect to $4 \cdot (X)_8$, it was predicted that $5 \cdot (X)_8$ will offer a higher affinity to smaller fullerenes.

Once $5 \cdot (BArF)_8$ was fully characterized, its ability to host fullerenes was tested starting with the encapsulation of C$_{60}$. Here, fast formation of 1:1 host:guest adducts was observed after mixing a 1:1 molar solution of $5 \cdot (BArF)_8$ in CH$_3$CN and C$_{60}$ in toluene. HRMS of the 1:1 C$_{60}$:$5 \cdot (BArF)_8$ mixture showed peaks corresponding exclusively to C$_{60}$□$5 \cdot (BArF)_8$ (Figure 1b and Figure S39). Data obtained from the UV-Vis titration of C$_{60}$ and $5 \cdot (BArF)_8$ fitted to a 1:1 binding model with an association constant of 1.29 (± 0.42)$\cdot 10^5$ M^{-1} (Figure S40).[23] The formation of the host:guest adduct was also evidenced in the ^{1}H-NMR spectrum, which showed several signals shifted; specially those corresponding to the aromatic protons of the phenyl rings of the porphyrin pointing inwards the cavity (Figure S41).

Afterwards, the encapsulation of C$_{70}$ was also attempted and monitored by HRMS. Remarkably, when a solution of C$_{70}$ in toluene was mixed with a solution of $5 \cdot (BArF)_8$ in CH$_3$CN in a 2:1 molar ratio (298 K, 48 h), peaks corresponding to C$_{70}$□$5 \cdot (BArF)_8$ adduct as well as peaks belonging to remaining empty capsule were observed (3:2 ratio respectively, see Figure S42). These results indicated a notable lower affinity of the capsule towards C$_{70}$ compared to C$_{60}$. UV-Vis titration with C$_{70}$ was in line with HRMS, since negligible changes on the Soret band were detected (Fig.S43).

The encapsulation of C$_{60}$ might seem surprising based solely on the short Porph-Zn···Porph-Zn distance measured in the crystal structure. This distance, 8.2 Å, is much smaller than the van der Waals diameter of C$_{60}$ (10.1 Å), thus indicating that $5 \cdot (BArF)_8$ must undergo important structural changes in solution to be able to accommodate C$_{60}$ (Figure 2a). The latter was explored through Molecular Dynamics (MD) simulations using CH$_3$CN as explicit solvent and Cl$^-$ as counterions (see Supporting Information for details). MD simulations revealed that the Porph-Zn···Porph-Zn distance in empty $5 \cdot (Cl)_8$ swings from 10.5 to 12.5 Å in solution (Figures 2b-2c and Video VS1 in the SI). On the other hand, MD simulations on C$_{60}$□$5 \cdot (Cl)_8$ and C$_{70}$□$5 \cdot (Cl)_8$ host-guest complexes showed a Porph-Zn···Porph-Zn distance of 12.3 - 13 Å for C$_{60}$ system and 12.6 - 13.3 Å for C$_{70}$ case (Figure S44). Porph-Zn···Porph-Zn distances explored during MD trajectory by C$_{70}$□$5 \cdot (Cl)_8$ are over the larger Porph-Zn···Porph-Zn distance measured by empty $5 \cdot (Cl)_8$ during MD, while C$_{60}$□$5 \cdot (Cl)_8$ distances are in breathing range (Figure 2b). Indeed, when comparing these Porph-Zn···Porph-Zn distances to those observed in the previously reported crystal structures of C$_{60}$□$4 \cdot (BArF)_8$ and C$_{70}$□$4 \cdot (BArF)_8$, 13.1 Å and 13.7 Å for C$_{60}$ and C$_{70}$ respectively,[21] the idea that C$_{70}$ fullerene is imposing a more severe distortion on the nanocapsule 5 than C$_{60}$ is reinforced. This

large distortion of the nanocapsule **5** required to encapsulate C_{70} is in agreement with the hampered encapsulation of C_{70} within **5**·$(BArF)_8$ and the higher selectivity towards C_{60}.

Encapsulation experiments with C_{60} were also performed by using **5**·$(CF_3SO_3)_8$ in the solid state. Interestingly, C_{60} was trapped after adding solid capsule to a solution of the fullerene in toluene (1:8 capsule:fullerene molar ratio) (Figure S45). Full formation of C_{60}☐**5**·$(CF_3SO_3)_8$ adduct was observed after 1 h stirring. Note here that the liquid/liquid complexation occurs faster (<5 min, 1:1 capsule:fullerene ratio) than the solid/liquid one. The slower rate of the solid/liquid encapsulation is most likely due to the higher rigidity of the capsule in the solid state, which restricts its dynamic adaptability needed to accommodate C_{60}, as revealed by MD simulations.

Taking advantage of the higher size-selectivity for C_{60}, nanocapsule **5**·$(BArF)_8$ was used to selectively separate C_{60} from fullerene extract (extract composition: 70% C_{60}, 28% C_{70}, 2% higher fullerenes). To this end, a solution of **5**·$(BArF)_8$ in CH_3CN was mixed with a solution of fullerene extract in toluene, in a 1:2 molar ratio (capsule:fullerenes). Delightfully, HRMS experiments showed that C_{60} was exclusively encapsulated from all the fullerenes mixture (Figure S46). No peaks corresponding to adducts with C_{70} or with other higher fullerenes present in the soot (i.e. C_{72}, C_{76} or C_{84}) were observed, even using extended reaction times. The same experiment was repeated using solid **5**·$(CF_3SO_3)_8$, in which C_{60} fullerene was also solely encapsulated (capsule:fullerene-extract in 1:8 molar ratio, see Figure S47). On the contrary, when larger **4**·$(BArF)_8$ capsule is added, either in solid or liquid form, to a fullerene extract solution both C_{60} and C_{70} and other higher fullerenes are encapsulated displaying no size selectivity.[21]
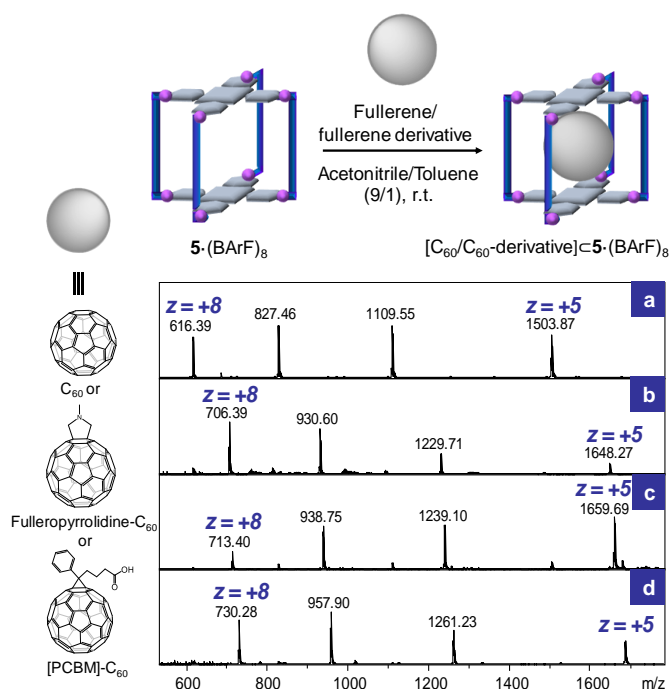

Figure 1. HRMS of **5**·$(BArF)_8$ and its host-guest adducts. HRMS in CH_3CN of (**a**) **5**·$(BArF)_8$, (**b**) C_{60}☐**5**·$(BArF)_8$, (**c**) [(mono)-N-pyrrolidine-C_{60}]☐**5**·$(BArF)_8$ and (**d**) [PCBM-C_{60}]☐**5**·$(BArF)_8$.
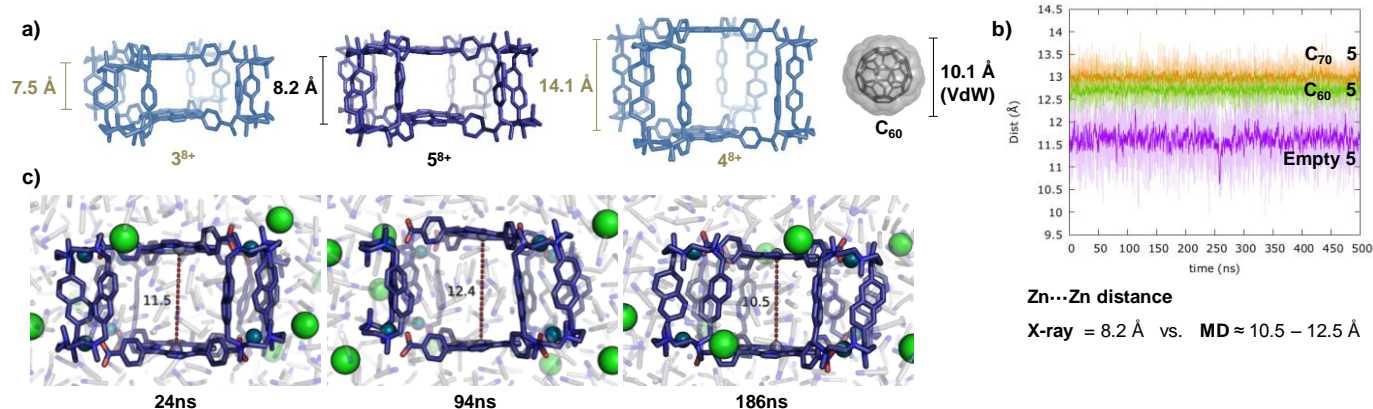
Figure 2. Crystal structures of the library of capsules 3^{8+}-5^{8+} and illustrations of MD simulation of capsule **5**. a) Lateral view of the crystal structures of $3 \cdot (ClO_4)_8$, $4 \cdot (BArF)_8$ and $5 \cdot (CF_3SO_3)_8$ (counter ions and hydrogen atoms are omitted for clarity). b) $Zn \cdots Zn$ distance measured along the 500 ns of Molecular Dynamics (MD) trajectory for $5 \cdot (Cl)_8$ (purple), $C_{60} \square 5 \cdot (Cl)_8$ (green) and $C_{70} \square 5 \cdot (Cl)_8$ (orange) in explicit CH_3CN solvent. For more clarity, the 10-step averaged value for each point is represented by the purple line in the plot. c) Representative snapshots taken along the MD trajectory to illustrate the conformational flexibility of 5^{8+}. $Zn \cdots Zn$ distances are given in Å, and hydrogen atoms are omitted for clarity.

Finally, the ability of $5 \cdot (BArF)_8$ to encapsulate C_{60} derivatives was also explored. Host-guest studies were carried out with PCBM-C_{60} and N-methylpyrrolidine-C_{60} (the latter was prepared as previously reported).[24] When a solution of the corresponding derivative in toluene was mixed with a solution of the capsule in acetonitrile in a 1:1 molar ration, clean formation of the host-guest complexes was observed by HRMS after 5 min stirring (Figure 1c-d, Figure S48-49). UV-Vis titration experiments were performed in order to estimate the association constant between $5 \cdot (BArF)_8$ receptor and the C_{60}-derivatives. Interestingly, the UV-Vis experiment following the formation of [N-methylpyrrolidine-C_{60}]$\square 5 \cdot (BArF)_8$ complex gave an association constant of $6.60 \ (\pm 0.32) \cdot 10^4 \ M^{-1}$ (2-fold smaller than the one obtained for C_{60}, Figure S50) and [PCBM-C_{60}]$\square 5 \cdot (BArF)_8$ complex gave an association constant of $1.27 \ (\pm 2.04) \cdot 10^5 \ M^{-1}$ (Figure S51) which is very similar to the one obtained for C_{60}. Encapsulation of both functionalized fullerenes was also performed by using $5 \cdot (CF_3SO_3)_8$ capsule in the solid state. Both species showed complete encapsulation after 1 h stirring a capsule suspension in a fullerene-derivative toluene solution (Figures S52 and S53);

however, encapsulation of PCBM-C_{60} was faster as it was evidenced by the HRMS spectrum recorded after 30 min reaction time compared to the one obtained for N-methylpyrrolidine-C_{60} (Figures S52 and S53). The latter observation is in agreement with the higher association constant obtained for PCBM-C_{60}.

A competition experiment between C_{60} fullerene and PCBM-C_{60} derivative, further supports the similar values obtained for their association constants. When 1 equivalent of **5**·(BArF)$_8$ capsule was mixed with 2.5 eq of C_{60} and 2.5 eq of PCBM-C_{60}, in toluene/acetonitrile (4/1) during 2.5h, very similar peaks on the HRMS were observed in line with the similar K_a (see Figure 3a and Figure S54). Interestingly, when a solution of 1 equivalent of **5**·(BArF)$_8$ capsule was mixed with 2.5 eq of C_{60} and 2.5 eq of N-methylpyrrolidine-C_{60}, in toluene/acetonitrile (4/1) during 2.5h, selective encapsulation of C_{60} occurred. The HRMS spectrum of the crude, displayed peaks corresponding to C_{60}□**5**·(BArF)$_8$ adduct and only residual peaks corresponding to N-methylpyrrolidine-C_{60}□**5**·(BArF)$_8$ adduct (Figure 3b, Figure S55 and S56 for comparable ionization behavior in HRMS). The notable difference between the association constants of C_{60} and C_{60}-fulleropyrrolidine derivative ($K_a(C_{60})/K_a(C_{60}$-fulleropyrrolidine) ~ 2), also enabled the separation of mono-Prato-C_{60} from the mixture with C_{60} using the previously described solid-washing strategy.[21] When a solid sample of **5**·(BArF)$_8$ containing both C_{60} and N-methylpyrrolidine-C_{60} was washed with CS_2, the Prato derivative was released while the C_{60} fullerene still remained trapped within the nanosapule (see Figure S57).
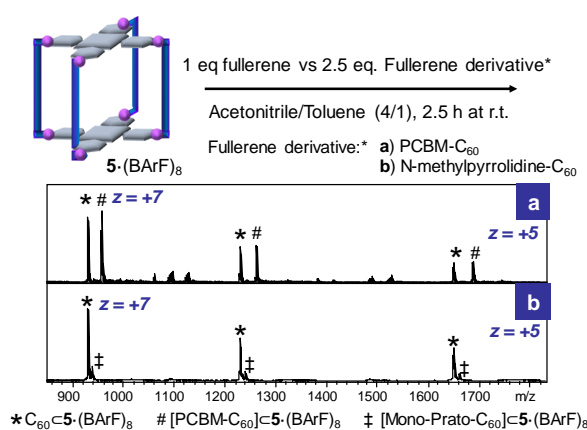

Figure 3. HRMS spectra of the competition experiments of a) C_{60} vs PCBM-C_{60} and b) C_{60} vs N-methylpyrrolidine-C_{60}.

Conclusions

Contraction of the organic macrocyclic ligands of the previously described **4**·(BArF)$_8$ capsule, led to the new tetragonal prismatic nanocapsule **5**·(BArF)$_8$. Remarkably, the size-selectivity imposed by the anisotropically contracted nanocapsule allows for the selective separation of C_{60} from fullerene extract

mixtures. Its capacity to host fullerenes and its size selectivity towards C_{60} can be rationalized by the dynamic adaptability that the capsule structure displays in solution, as shown by MD simulations. **5**·(BArF)$_8$ also encapsulates C_{60}-PCBM and N-methyl-pyrrolidine-C_{60}, displaying a larger affinity for C_{60} than for the latter Prato derivative, allowing its selective purification. Nanocapsule **5**·(BArF)$_8$ sets the knowledge basis for future purification of C_{60}-derivative mixtures.

Notes and references

1   C. García-Simón, R. Gramage-Doria, S. Raoufmoghaddam, T. Parella, M. Costas, X. Ribas and J. N. H. Reek, *J. Am. Chem. Soc.*, 2015, **137**, 2680–2687.

2   C. Zhao, F. D. Toste, K. N. Raymond and R. G. Bergman, *J. Am. Chem. Soc.*, 2014, **136**, 14409–14412.

3   K. Yamashita, M. Kawano and M. Fujita, *Chem. Commun.*, 2007, **1**, 4102–4103.

4   T. R. Cook, Y.-R. Zheng and P. J. Stang, *Chem. Rev.*, 2013, **113**, 734–777.

5   J. J. Henkelis and M. J. Hardie, *Chem. Commun.*, 2015, **51**, 11929–11943.

6   H. W. Kroto, J. R. Heath, S. C. O'Brien, R. F. Curl and R. E. Smalley, *Nature*, 1985, **318**, 162–163.

7   J. J. Ryan, H. R. Bateman, A. Stover, G. Gomez, S. K. Norton, W. Zhao, L. B. Schwartz, R. Lenk and C. L. Kepley, *J. Immunol.*, 2007, **179**, 665–672.

8   J. Xiao and M. E. Meyerhoff, *J. Chromatogr. A*, 1995, **715**, 19–29.

9   Y. Matsuo, A. Iwashita, Y. Abe, C. Li, K. Matsuo, M. Hashiguchi and E. Nakamura, *J. Am. Chem. Soc.*, 2008, **130**, 15429–15436.

10   G. Dennler, M. C. Scharber and C. J. Brabec, *Adv. Mater.*, 2009, **21**, 1323–1338.

11   C. Garcia-Simon, M. Costas and X. Ribas, *Chem. Soc. Rev.*, 2016, **45**, 40–62.

12   M. Zhang, H. Xu, M. Wang, M. L. Saha, Z. Zhou, X. Yan, H. Wang, X. Li, F. Huang, N. She and P. J. Stang, *Inorg. Chem.*, 2017, **56**, 12498–12504.

13   C. Colomban, G. Szalóki, M. Allain, L. Gómez, S. Goeb, M. Sallé, M. Costas and X. Ribas, *Chem. Eur. J.*, 2017, **23**, 3016–3022.

14   T. K. Ronson, W. Meng and J. R. Nitschke, *J. Am. Chem. Soc.*, 2017, **139**, 9698–9707.

15   K. Tashiro and T. Aida, *Chem. Soc. Rev.*, 2007, **36**, 189–197.

16   W. Meng, B. Breiner, K. Rissanen, J. D. Thoburn, J. K. Clegg and J. R. Nitschke, *Angew. Chem. Int. Ed.*, 2011, **50**, 3479–3483.

17   C. Zhang, Q. Wang, H. Long and W. Zhang, *J. Am. Chem. Soc.*, 2011, **133**, 20995–21001.

18   E. V. Peris, D. Gusev and V. Martínez-Agramunt, *Chem. Eur. J.*, , DOI:10.1002/chem.201803034.

19   Y. Shi, K. Cai, H. Xiao, Z. Liu, J. Zhou, D. Shen, Y. Qiu, Q. Guo, C. Stern, M. R. Wasielewski, F. Diederich, W. A. Goddard and J. F. Stoddart, *J. Am. Chem. Soc.*, 2018, DOI:10.1021/jacs.8b08555.

20   N. Kishi, Z. Li, K. Yoza, M. Akita and M. Yoshizawa, *J. Am. Chem. Soc.*, 2011, **133**, 11438–41.

21   C. García-Simón, M. Garcia-Borràs, L. Gómez, T. Parella, S. Osuna, J. Juanhuix, I. Imaz, D. Maspoch, M. Costas and X. Ribas, *Nat. Commun.*, 2014, **5**, 5557.

22   C. García-Simón, M. Garcia-Borràs, L. Gómez, I. Garcia-Bosch, S. Osuna, M. Swart, J. M. Luis, C. Rovira, M. Almeida, I. Imaz, D. Maspoch, M. Costas and X. Ribas, *Chem. Eur. J.*, 2013, **19**, 1445–1456.

23   D. Brynn Hibbert and P. Thordarson, *Chem. Commun.*, 2016, **52**, 12792–12805.

24   M. Maggini and M. Prato, *J. Am. Chem. Soc.*, 1993, **115**, 9798–9799.